Pharmacological Research 207 (2024) 107336

Contents lists available at ScienceDirect

Pharmacological Research

journal homepage: www.elsevier.com/locate/yphrs

Inhibition of K63 ubiquitination by G-Protein pathway suppressor 2 (GPS2) regulates mitochondria-associated translation

Yuan Gao [a,1], Julian Kwan [a,b], Joseph Orofino [a], Giulia Burrone [a,e,f,g], Sahana Mitra [a], Ting-Yu Fan [a], Justin English [a,c], Ryan Hekman [a,b], Andrew Emili [a,b,d], Shawn M. Lyons [a], Maria Dafne Cardamone [a], Valentina Perissi [a,*]

[a] Department of Biochemistry and Cell Biology, Chobanian&Avedisian School of Medicine, Boston University, Boston, MA 02115, United States
[b] Center for Network and Systems Biology, Boston University, Boston, MA 02115, United States
[c] Graduate Program in Pharmacology and Experimental Therapeutics, Chobanian&Avedisian School of Medicine, Boston University, Boston, MA 02115, United States
[d] Biology Department, Boston University, Boston, MA 02115, United States
[e] Department of Computer Science, University of Torino, Torino, Italy
[f] Department of Clinical and Biological Science, University of Torino, Torino, Italy
[g] Graduate Program in Complex Systems for Quantitative Biomedicine, University of Torino, Torino, Italy

ARTICLE INFO

Keywords:
Ubiquitin
GPS2
Mitochondria
PABPC1
Translation
Mitochondria stress response (MSR)

Chemical compounds studied in this article:
FCCP
Homo-harringtonine
NSC697923
Puromycin
Tamoxifen

ABSTRACT

G-Protein Pathway Suppressor 2 (GPS2) is an inhibitor of non-proteolytic K63 ubiquitination mediated by the E2 ubiquitin-conjugating enzyme Ubc13. Previous studies have associated GPS2-mediated restriction of ubiquitination with the regulation of insulin signaling, inflammatory responses and mitochondria-nuclear communication across different tissues and cell types. However, a detailed understanding of the targets of GPS2/Ubc13 activity is lacking. Here, we have dissected the GPS2-regulated K63 ubiquitome in mouse embryonic fibroblasts and human breast cancer cells, unexpectedly finding an enrichment for proteins involved in RNA binding and translation on the outer mitochondrial membrane. Validation of selected targets of GPS2-mediated regulation, including the RNA-binding protein PABPC1 and translation factors RPS1, RACK1 and eIF3M, revealed a mitochondrial-specific strategy for regulating the translation of nuclear-encoded mitochondrial proteins via non-proteolytic ubiquitination. Removal of GPS2-mediated inhibition, either via genetic deletion or stress-induced nuclear translocation, promotes the import-coupled translation of selected mRNAs leading to the increased expression of an adaptive antioxidant program. In light of GPS2 role in nuclear-mitochondria communication, these findings reveal an exquisite regulatory network for modulating mitochondrial gene expression through spatially coordinated transcription and translation.

1. Introduction

Maintenance of mitochondria metabolism and energy homeostasis is guaranteed by a constant turnover of the mitochondrial network, including both generation of new mitochondria, remodeling of existing mitochondria and removal of damaged organelles [1]. Mitochondrial biogenesis and rewiring of mitochondrial functions require coordinated gene expression from the mitochondrial and nuclear genomes [2–5]. This coordination is achieved through energy-sensing signaling pathways impacting on the transcriptional network controlling the expression of nuclear-encoded mitochondrial genes, and via shuttling of transcription factors and cofactors between the two organelles [6–9]. In yeast, balanced expression of different OXPHOS subunits is also facilitated by synchronized control of mitochondrial and cytosolic translation

Abbreviations: CE, Cytosolic Extracts; DEGs, Differentially Expressed Genes; DEPs, Differentially Expressed Proteins; GPS2, G-Protein Pathway Suppressor 2; HHT, Homo-harringtonine; HMW, High Molecular Weight; K63, Lysine 63; KO, Knock-Out; LC-MS, Liquid Chromatography Mass Spectrometry; LMW, Low Molecular Weight; ME, Mitochondrial Extracts; MEF, Mouse Embryonic Fibroblast; NE, Nuclear Extracts; neMITO, nuclear encoded mitochondrial genes; OMM, Outer Mitochondrial Membrane; OXPHOS, Oxidative Phosphorylation; PABPC1, Poly-A Binding Protein C1; PAIP1/2, PABP-interacting protein 1/2; PTM, Post Translational Modification; SILAC, Stable Isotope Labeling with Amino acids in cell Culture; TMT, Tandem Mass Tag; Ub, Ubiquitin; WCE, Whole Cell Extracts; WT, Wild Type.

* Corresponding author.
E-mail address: vperissi@bu.edu (V. Perissi).
[1] Current address: College of Horticulture, Nanjing Agricultural University, Nanjing 210095, China.

https://doi.org/10.1016/j.phrs.2024.107336
Received 2 January 2024; Received in revised form 29 July 2024; Accepted 29 July 2024
Available online 31 July 2024

[10–13]. This underscores that the maintenance of mitochondrial homeostasis is achieved through coordinated regulation of multiple levels of gene expression. However, the molecular mechanisms promoting balanced mitochondrial gene expression via regulated mRNA processing and translation at the level of single organelles in mammals are not yet fully understood. In particular, a mechanistic understanding of the modes of regulation of mitochondria-associated translation is currently lacking, even though recent studies have provided clues to the specificity of translation on mitochondria-associated ribosomes, as compared to cytosolic ribosomes, through the identification of RNA-binding proteins responsible for recruiting selected mRNAs to the mitochondrial outer membrane surface [14–22].

Ubiquitination is a reversible protein post-translational modification that is achieved through the sequential actions of several classes of enzymes, including a ubiquitin (Ub)-activating enzyme (E1), a Ub-conjugating enzyme (E2), and a Ub ligase (E3), working together to mediate the attachment of one or multiple ubiquitin moieties to lysine residues on target proteins [23,24]. In the case of poly-ubiquitination, chains of different topology can either promote protein degradation or serve, as in the case of other post-translational modifications, to influence protein functions and interactions [25,26]. Among others, K48-linked ubiquitin chains are best known as markers for proteasomal degradation, whereas K63-linked ubiquitin chains are non-proteolytic [27,28] and have been associated with the regulation of immune signaling, DNA damage repair, protein sorting, and translation [29–36]. Moreover, recent studies showing that K63-linked ubiquitin mediates translational regulation in yeast exposed to oxidative stress suggest that K63Ub may play a broad role in regulating cellular metabolism and adaptive responses to stress [37–42].

Our previous work revealed that GPS2 acts as a checkpoint regulator for K63 ubiquitination events mediated by the E2 conjugating enzyme UBE2N (also called Ubc13) and associated E3 ligases TRAF6 and RNF8 [43]. GPS2-mediated inhibition of K63 ubiquitination is essential for promoting several coordinated functions across the cell, including the transcriptional regulation of mitochondrial genes in the nucleus and post-translational regulation of insulin signaling and pro-inflammatory pathways in the cytosol [9,44–46]. These complementary activities across different subcellular compartments are facilitated by GPS2 translocation between organelles. In particular, previous studies show that mitochondria-to-nucleus shuttling of GPS2 during adipocyte differentiation controls mitochondria biogenesis via transcriptional activation of nuclear-encoded mitochondrial (neMITO) genes [9]. Mitochondria-to-nucleus translocation of GPS2 upon mitochondrial depolarization is similarly required for licensing the expression of nuclear stress-response genes [9]. While these studies establish a clear role for GPS2 in regulating mitochondrial functions through modulation of nuclear gene expression upon retrograde translocation, it remains to be determined whether the removal of GPS2 itself from mitochondria plays any role in the process. Here, we have profiled the GPS2-regulated K63 ubiquitome in different cell types and asked to what extent GPS2 removal from mitochondria, either by deletion or through stress-induced retrograde translocation, licenses the ubiquitination of mitochondrial targets. This approach revealed a novel regulatory strategy for modulating the translation of selected neMITO transcripts via K63 ubiquitination of mitochondria-associated translation factors, thus identifying GPS2 as a key player for mediating the coordination of nuclear and extranuclear processes contributing to the remodeling of cellular metabolism.

2. Results

2.1. Profiling of GPS2-regulated ubiquitome in mouse embryonic fibroblast

Our previous work indicates that GPS2 translocates from mitochondria to nucleus, where it regulates the transcription of neMITO and stress response genes [9]. However, the function – if any – of GPS2 while residing on the outer mitochondrial membrane (OMM) remains unknown. Based on previous work indicating that GPS2 exerts nuclear and cytosolic functions by inhibiting the ubiquitin-conjugating enzyme Ubc13/UBE2N [9,43–47], we hypothesized that the removal of GPS2 via retrograde signaling would license K63 ubiquitination of targets on the outer mitochondrial surface. To investigate this hypothesis, we compared immortalized mouse embryonic fibroblast cells (MEFs) derived from either GPS2$^{fl/fl}$/Ubc^{ERT2}-Cre^{+} or GPS2$^{fl/fl}$/Ubc^{ERT2}-Cre^{-} mice. Upon tamoxifen treatment, GPS2 deletion is induced in Ubc^{ERT2}-Cre^{+} cells (from here on called GPS2-KO), whereas Ubc^{ERT2}-Cre^{-} (from here on called WT) serve as negative control (Fig. 1A). In agreement with previous reports [9,48], we observed a significant reduction in mitochondrial content in GPS2-KO cells (Supplement Figure S1A). To assess the impact of GPS2 deletion on mitochondria-associated ubiquitination, we performed western blotting for total ubiquitin or K63 ubiquitin chains on equal amounts of fractionated extracts, observing a pronounced increase in the abundance of K63 ubiquitinated proteins in mitochondrial extracts (ME) from GPS2 KO cells as compared to WT cells (Fig. 1A). In agreement with the increased abundance of K63 ubiquitin chains, we also observed elevated levels of the ubiquitin-binding autophagy receptors p62/SQSTM1 and OPTN1 (Fig. 1B). Moreover, in accord with GPS2 transcriptional role as a coactivator for nuclear-encoded mitochondrial genes, mtHSP70 expression was found lower in KO compared to WT cells [9] (Fig. 1B).

To identify the targets of GPS2-regulated ubiquitination, we profiled the K63 ubiquitome in GPS2 WT and KO MEFs by LC-MS/MS. Relative quantification was performed by stable isotope labeling with amino acids in cell culture (SILAC) (Supplemental Figure S1B). K63 ubiquitinated proteins were enriched prior to mass spectrometry using the high-affinity lysine-63-poly-ubiquitin binding domain Vx3K0 [49], which was confirmed to bind to K63 but not to K48 ubiquitin chains (Supplemental Figure S1C). Equal amounts of whole cell extracts from GPS2 WT and KO cells were mixed and then immunoprecipitated by Vx3K0 (Supplemental Figure S1D). The purified proteins were then digested by trypsin and analyzed via mass spectrometry. Despite the modest increase in the amount of K63 ubiquitinated proteins recovered from GPS2 KO cells at the whole cell level, as compared to WT and seen by western blotting (Fig. 1**C**), profiling by LC-MS/MS led to the identification of 73 candidate targets, out of 230 proteins identified in both experiments, for which the increase in the H/L ratio consistently observed across two biological replicates indicated increased ubiquitination and/or increased interaction with ubiquitinated targets in GPS2-KO cells (Fig. 1D top right quadrant, Supplemental Figure S1D and Supplemental Table 1A&1B). To further validate our findings, we also performed K63-Ubiquitome profiling using TMT labeling instead of SILAC (Supplemental Figure S1F and Supplemental Table 1C). With this more sensitive approach we recovered 121 upregulated targets among 234 significantly changed proteins with a P-value$<$0.05 (Supplemental Table 1C).

To our initial surprise, none of these datasets displayed an enrichment for mitochondrial proteins nor for targets of the E3 ligase Parkin [50], which is known to promote K63 ubiquitination of mitochondrial proteins recognized by OPTN and p62/SQSTM [51] (Fig. 1E and Supplemental Table S1C). This result suggested that the accumulation of K63 ubiquitinated proteins observed upon GPS2 deletion in non-stressed conditions is distinct from the program associated with Parkin-induced activation of mitophagy in response to mitochondrial stress. To further characterize the GPS2-regulated program, we conducted KEGG pathway enrichment analysis of GPS2 candidate targets to identify the biological pathways most impacted by GPS2-regulated ubiquitination. Unexpectedly, we found that putative targets of GPS2-mediated regulation identified by SILAC were strongly enriched for factors involved in protein translation (Fig. 2A). Comparable results were obtained using the dataset obtained by TMT labeling (Supplemental Figure S2A and Supplemental Table 1C). A similar enrichment in proteins involved in

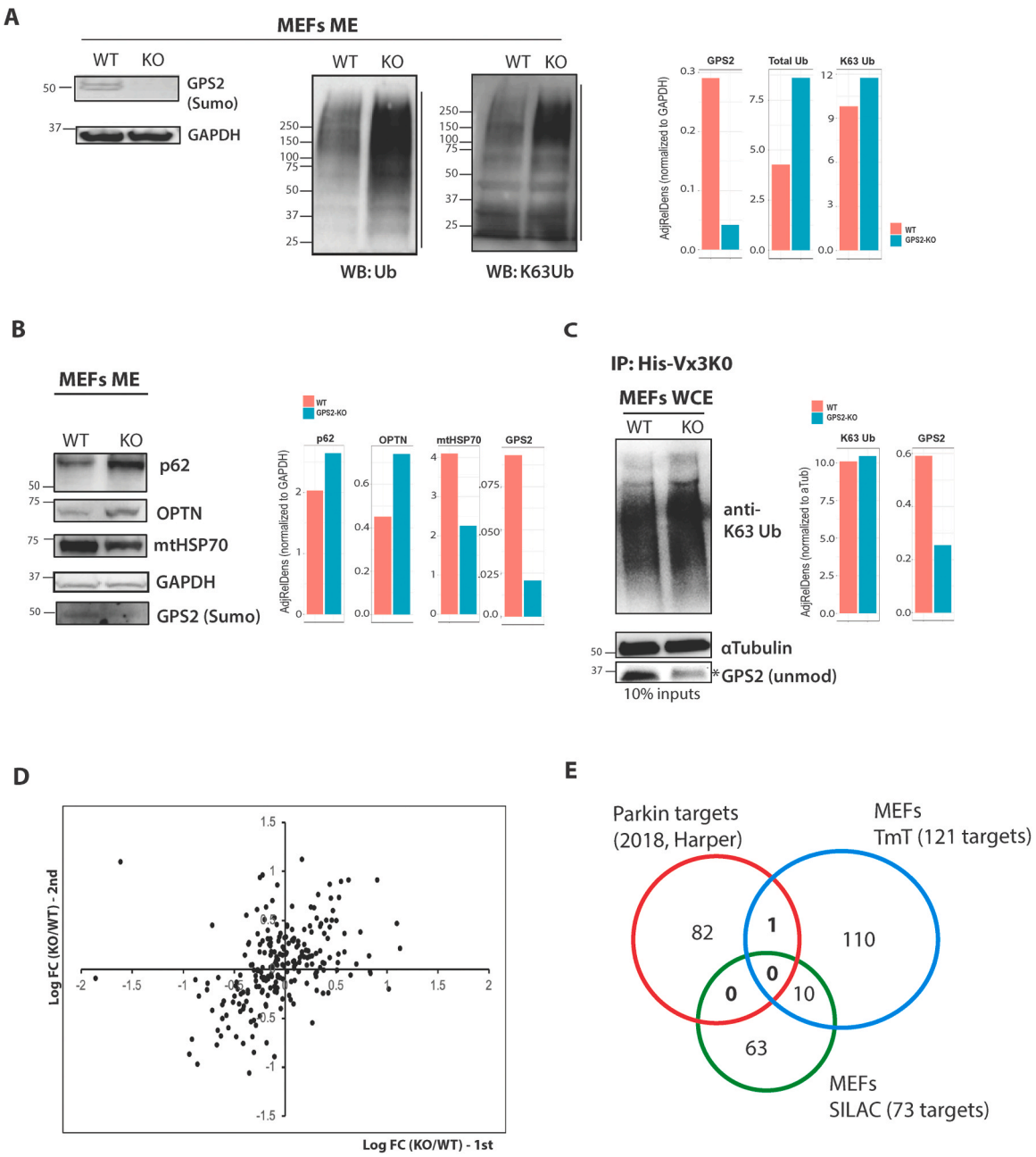

Fig. 1. K63 ubiquitome profiling of GPS2 WT and KO MEFs by LC-MS/MS. A, Increased K63 ubiquitination in MEFs mitochondrial extracts (ME) in GPS2 KO compared to WT by western blot. Quantification of each individual gel by ORCA is normalized for the mitochondria-associated housekeeping gene GAPDH [91,92] as the expression of classic mitochondrial markers is impacted by GPS2 deletion (see Cardamone et al. [9] and mtHSP70 blot in Fig1B). Note that GPS2 in ME runs at higher molecular weight than expected size of 36kD due to sumoylation on residues K45 and K71, as described before[9]. B, Increased expression of ubiquitin receptors P62 and OPTN in ME from GPS2 KO as compared to WT by western blot. Quantification of the blot by ORCA is normalized to the housekeeping gene GAPDH. C, WB analysis of K63 ubiquitinated proteins captured by Vx3K0 using equal amounts of whole cell extracts (WCE) from GPS2 WT and KO MEFs. Quantification of the blot by ORCA is normalized to the housekeeping gene alpha-tubulin. Note that in WCE GPS2 is most abundant as an unmodified protein with the expected MW of 36KD. Fractionated extracts are required to visualize the sumoylated fraction of GPS2 that is found associated with the mitochondria and to confirm full clearance of GPS2 in KO cells due to a non-specific band running at the same MW as GPS2 (* band remaining after GPS2 deletion). D, Scatter plotting analysis of SILAC data obtained in two independent experiments. The KO/WT SILAC ratio of two labeled samples were converted to log2 scale for analysis. The proteins identified by SILAC-K63 ubiquitome and their SILAC ratios are listed in supplemental Table 1 A. E, Venn diagram comparing identified putative targets of GPS2-regulated K63 ubiquitination including both SILAC and TMT datasets, and Parkin targets reported by Ordureau et al., 2018 [50]. Protein datasets and overlaps are listed in supplemental Table 1 C.

translation and RNA processing was also observed by profiling the K63 ubiquitome of triple negative MDA-MB-231 breast cancer cells with GPS2 deletion [46] (Supplemental Figure S2B and Supplemental Table 1C).

Among the candidate targets of GPS2-mediated regulation, we selected the single candidate protein consistently identified across different experimental setups (SILAC and TMT labeling) and distinct cell types (MEFs and MDA-MB-231) for further investigation (Fig. 2B, Supplemental Table 1A&1C). The RNA binding protein PABPC1 was previously reported to be ubiquitinated in the context of translation quality

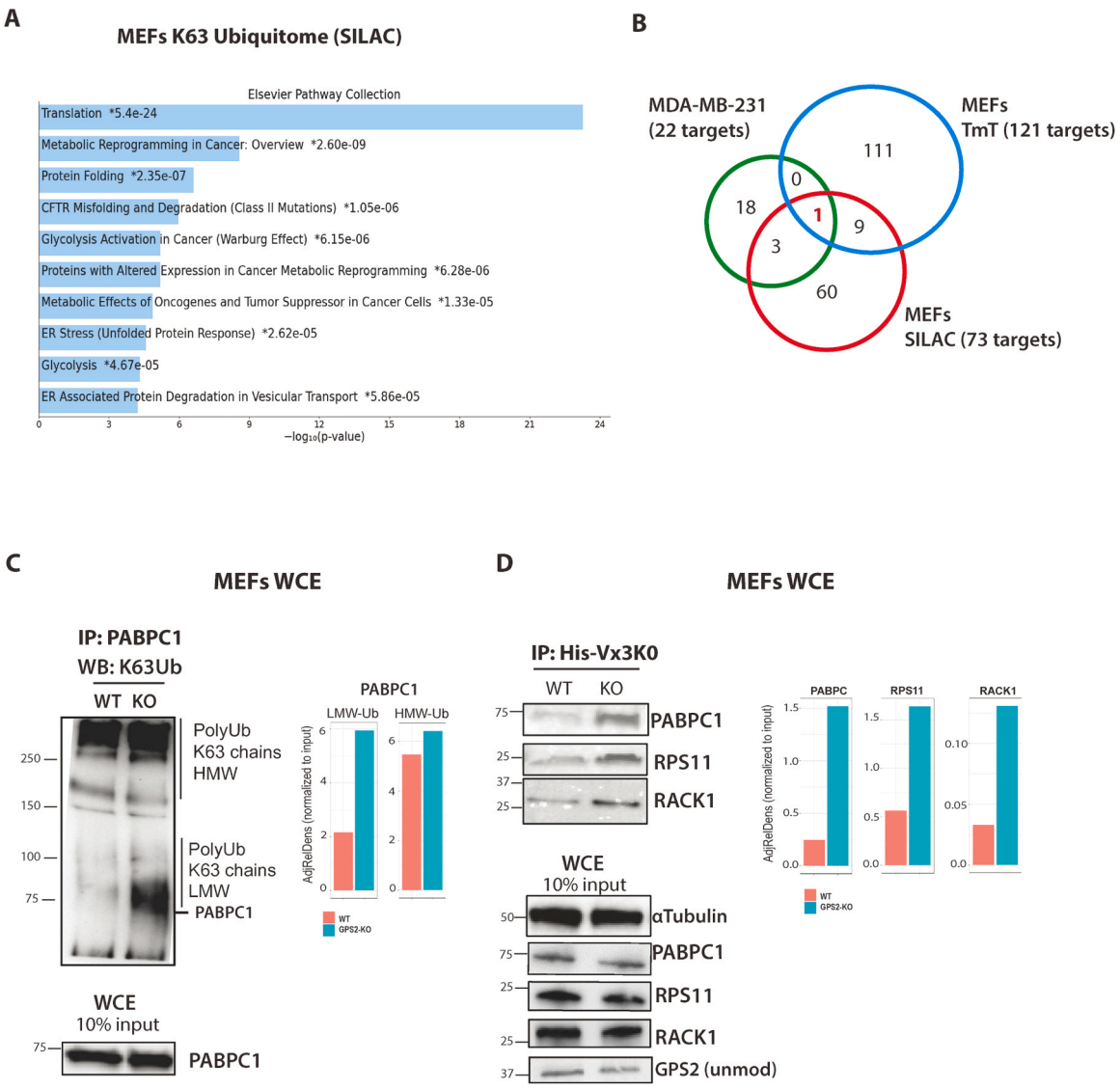

Fig. 2. Ubiquitination of candidate RNA binding proteins and translation factors regulated by GPS2. A, Gene ontology analysis of putative targets of GPS2-regulated K63 ubiquitination identified by SILAC labeling in MEFs. B, Venn diagram comparing putative targets of GPS2-regulated K63 ubiquitination identified in MEFs (either by SILAC or TMT labeling) and MDA-MB231 cells. C, Detection of K63 ubiquitination by IP/WB of PABPC1 in whole cell extracts from GPS2 WT and KO MEFs shows an increase in the amount of K63 associated, directly or indirectly, with PABPC1. Quantification of the blot by ORCA is normalized to PABPC1 input. D, Detection of PABPC1, RPS11 and RACK1 by IP/WB with the K63-ubiquitin binding domain Vx3K0 in whole cell extracts from GPS2 WT and KO MEFs. Quantification by ORCA for each blot is normalized to the corresponding input.

control [52]. We used two complementary IP/WB approaches to validate PABPC1 as a target of GPS2-mediated regulation in MEF cells. First, we immunoprecipitated PABPC1 from either WT or GPS2-KO cellular extracts and visualized associated ubiquitin chains by WB. As expected, removal of GPS2-mediated inhibition led to an increase in the abundance of K63 Ub chains associated with PABPC1 (Fig. 2C). Remarkably, the increase was more evident in the 75–100 kDa range which corresponds to the expected size for PABPC1 modified by the addition of 3–4 Ub molecules (Fig. 2C, see quantification). Next, we isolated K63 Ub-containing proteins from whole-cell extracts using the Vx3K0 UBD and quantified the relative amount of PABPC1 immunoprecipitated in the two conditions by WB (Fig. 2D). While the large increase in the amount of PABPC1 that was isolated based on K63-Ub binding in GPS2-KO cells as compared to WT confirmed the mass spectrometry results, this approach did not allow to visualize poly-ubiquitinated PABPC1. While this result could indicate that the unmodified PABPC1 was isolated based on indirect binding to other ubiquitinated targets, it is also possible that only a small fraction of the total protein amount gets ubiquitinated thus making it technically challenging to visualize the modified form. Notably, comparable results were obtained for other two putative targets, the translation factors RPS11 and RACK1 (Fig. 2D), which had been previously reported as direct targets of non-proteolytic ubiquitination [40,53]. [40,53]

2.2. Regulation of mitochondria-associated protein translation

Together these results indicated that the increase in the amount of non-proteolytic K63 ubiquitination caused by GPS2 deletion impacted proteins involved in regulating translation. To investigate whether the increased ubiquitination had functional consequences, we asked whether protein translation is affected by the absence of GPS2. To assess translation efficiency across subcellular compartments, we monitored the incorporation of puromycin into newly synthesized proteins in both whole cell and fractioned extracts from WT and KO cells. Pre-treatment with the translation initiation inhibitor homoharringtonine (HHT) [54] reduced puromycin incorporation, confirming that the signal observed

corresponded to active translation. While no differences between WT and KO were observed at the whole cell level (Fig. 3A), a robust increase in puromycin incorporation was observed in mitochondrial extracts from GPS2-KO cells compared to WT (Fig. 3B). The increase in puromycin incorporation observed in the mitochondrial compartment, differed greatly in comparison to other compartments, with no changes observed in the nucleus and only a slight increase in the cytosol (Supplemental Figure S3A & B). This suggested that mitochondria-associated translation may be specifically affected by the absence of GPS2. As an alternative approach to investigate the impact of GPS2 deletion on mitochondria-associated translation, we assessed the formation of the closed-loop promoting mRNA circularization and translation via interactions between PABPC1 and the polyA-containing 3'UTR and 5' Cap-bound components of the translation initiation complex [55,56]. In agreement with the previous results, co-immunoprecipitation experiments indicated that PABPC1 interaction with the translation initiation factor eIF4G and translational activator PABP-interacting protein 1 (PAIP1) is more robust in mitochondria from GPS2-KO cell than their WT counterparts (Fig. 3C). In contrast, interaction with the translational repressor PABP-interacting protein 2 (PAIP2), which competes with PAIP1 for interaction with PABP [57], is decreased (Fig. 3C). These differences appear specific to the mitochondrial compartment as they

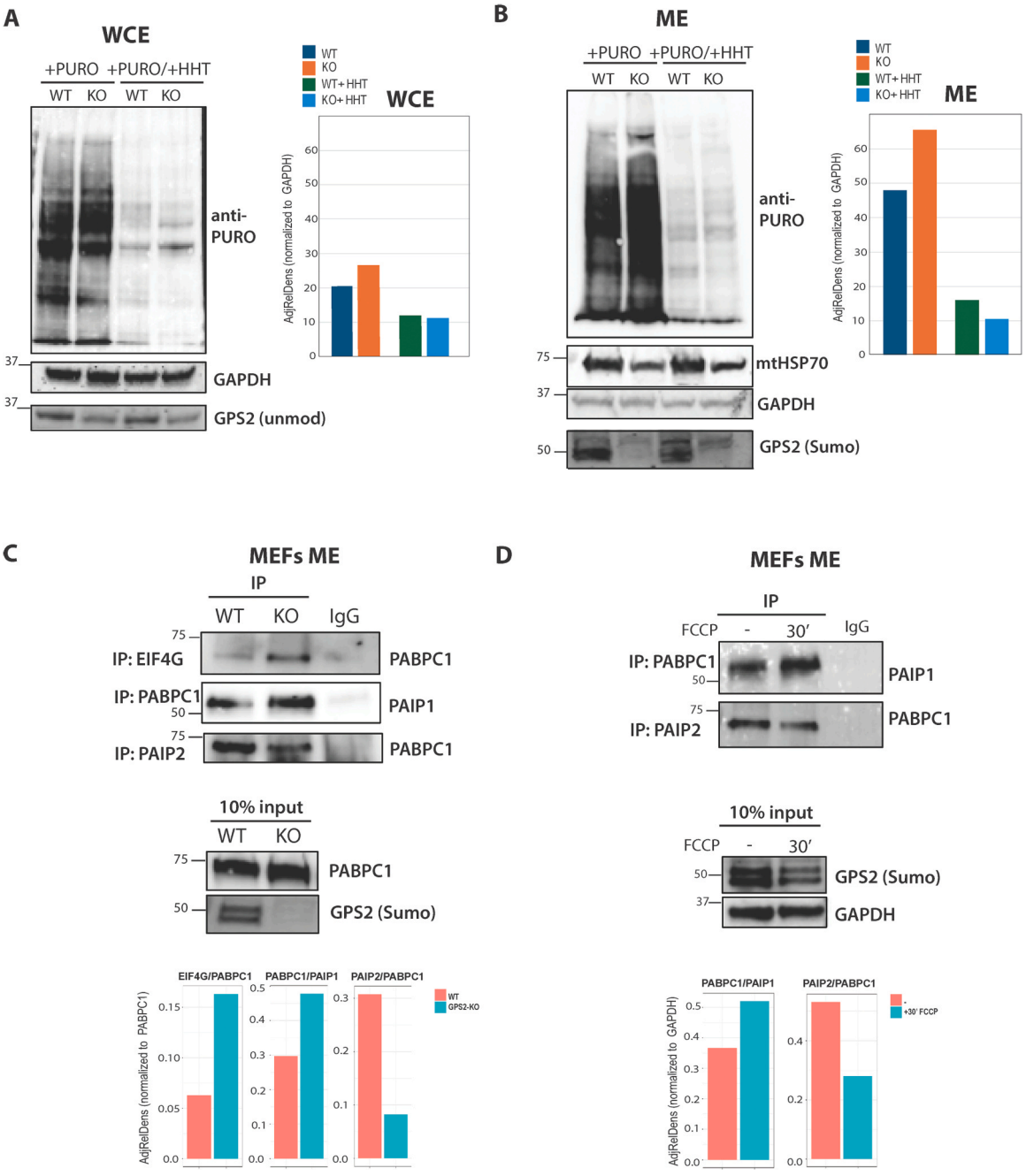

Fig. 3. Mitochondria-associated translation is enhanced in the absence of GPS2. A, Puromycin labeling of *de novo* protein synthesis in whole cell extracts (WCE) pretreated w/o homoharringtonine (HHT). Cells were treated with HHT for 10 min prior to treatment with 0.9 mM puromycin for additional 5 min. Quantification of the blot by ORCA is normalized to GAPDH. B, Puromycin labeling of *de novo* protein synthesis in mitochondrial extracts (ME) pretreated w/o homoharringtonine (HHT) as in A. Quantification of the blot by ORCA is normalized to GAPDH. C, IP/WB analysis assessing binding of PABPC1 with EIF4G, PAIP1 and PAIP2 in mitochondrial extracts (ME) from GPS2 WT and KO MEFs. Quantification of each blot by ORCA is normalized to the PABPC input. D, IP/WB analysis assessing binding of PABPC1 with PAIP1 and PAIP2 in MEFs mitochondrial extracts upon FCCP treatment. Quantification of the blot by ORCA is normalized to GAPDH.

are not observed when probing cytosolic extracts (Supplemental Figure S3C). As previous studies indicate that measurement of puromycin incorporation selectively assesses the translation of nuclear-encoded mitochondrial transcripts on the OMM as compared to the translation of mitochondria-encoded genes within the mitochondria [58], these results not only indicate that the removal of GPS2 is associated with an increase in mitochondria-associated translation, but are also indicative of a localized regulatory strategy impacting the mRNAs that are translated by ribosomes docked on the mitochondria. Such a localized regulatory strategy is consistent with GPS2 localization on the OMM and would provide an opportunity for regulating mitochondria-associated translation via retrograde shuttling of GPS2 from mitochondria to the nucleus. Thus, we investigated whether mitochondria-associated translation is responsive to mitochondrial stressors promoting GPS2 relocalization to the nucleus. Specifically, we assessed whether translation efficiency improved upon depolarization of mitochondria by FCCP, a condition previously shown to induce the removal of GPS2 from the OMM through retrograde translocation to the nucleus [9] (Supplemental Figure S3D**,** note that mitochondrial GPS2 is almost entirely sumoylated as described before [9]). As shown in Fig. 3D, the interaction between PABPC1 and the translation initiation complex in mitochondrial extracts increased in response to FCCP treatment, similar to what previously observed in GSP2-KO cells, thus confirming that mitochondria-associated protein translation is upregulated across different experimental conditions causing GPS2 removal from the OMM.

2.3. Ubiquitination of mitochondria-associated translation factors

Next, we focused on the mechanism of GPS2-mediated regulation of mitochondria-associated translation. For the localized increase in protein translation observed in GPS2-KO cells to be regulated by unrestricted K63 ubiquitination in the absence of GPS2, the translation factors identified as putative targets of GPS2 regulation should be ubiquitinated within the mitochondrial compartment. In support of this hypothesis, larger amounts of PABPC1, RPS11 and RACK1 were isolated based on K63-Ub binding of in fractionated mitochondrial extracts from GPS2-KO cells as compared to WT (Fig. 4A and Supplemental Figure 4A). More importantly, poly-ubiquitinated PABPC1 could be detected in the mitochondrial extract of GPS2-KO cells by WB with PABPC1 antibody (Fig. 4A), thus confirming that PABPC1 is directly ubiquitinated even though the ubiquitination affects only a small fraction of the total protein pool in the cell. A similar increase in the ubiquitination of PABPC1 within the mitochondrial compartment was observed upon FCCP treatment, again confirming that removal of GPS2 from mitochondria leads to comparable phenotypes whether it is achieved through genetic deletion or depolarization-induced translocation to the nucleus (Fig. 4B). To further confirm the topology of ubiquitin chains associated with mitochondrial PABPC1, we also immunoprecipitated PABPC1 from mitochondrial extracts of WT cells treated with FCCP and probed for K63 ubiquitin. As shown in Fig. 4C, K63 ubiquitination of PABPC1 rapidly increased upon mitochondrial depolarization in parallel to GPS2 retrograde translocation to the nucleus and is impaired upon transient downregulation of the K63 ubiquitin-conjugating enzyme Ubc13 or the OMM-anchored E3 ubiquitin ligase MUL1 [59–61], which is the only mitochondria-associated ligase known to mediate the synthesis of K63 ubiquitin chains beyond Parkin (Supplemental Figure 4B & 4C). Moreover, inhibiting the activity of Ubc13 with the chemical inhibitor NSC697923 is sufficient to reverse the shift from LMW to HMW K63Ub chains observed in GPS2 KO cells (Supplemental Figure 4D). Together these results indicate that PABPC1 is polyubiquitinated with K63 ubiquitin chains in the mitochondria, and that the ubiquitination increases upon mitochondrial depolarization by FCCP. To further assess the machinery responsible for mediating K63 ubiquitination of PABPC1, we reconstituted the ubiquitination reaction *in vitro* using recombinant His-PABPC1 and E1, E2 (Ubc13/Uev1a), E3 (MUL1) enzymes. Ubiquitination assays confirmed that PABPC1 is poly-ubiquitinated by MUL1/Ubc13 *in vitro* (Figs. 4D and 4E), and that the reaction is inhibited by GPS2 (Fig. 4E). Also, the topology of the chains was confirmed *in vitro* by use of K63R mutant ubiquitin which is unable to form poly-ub chains (Fig. 4F), even though probing the reaction by western blotting for PABPC1 indicated that only a small fraction of the protein gets ubiquitinated (See long exposure in Supplemental Figure 4E). To further confirm the ubiquitination of PABPC1 *in vitro* and distinguish between the ubiquitination of PABPC1 and background signal due to free standing chains and auto-ubiquitinated MUL1 (see Fig. 4D, left panel), we also compared the ubiquitination profile of WT PABPC1 and that of a mutant version of PABPC1 lacking all previously reported ubiquitination sites (K78, K188, K284, and K512) [52]. As shown in Supplemental Figure 4F, the ubiquitination observed with the 4 K mutant is comparable to the background, thus confirming that the additional signal observed in presence of WT PABPC1 corresponds to poly-ubiquitinated PABPC1.

Most importantly, downregulation of the E3 ubiquitin ligase MUL1 [59–61] was sufficient to rescue the increase in translation efficiency and closed-loop formation observed in the absence of GPS2 (Fig. 4G & 4H), thus indicating that ubiquitination activity is required for promoting the increase in mitochondria translation and that GPS2 regulates mitochondria-associated translation by preventing aberrant activity of the Mul1/Ubc13 ubiquitination complex. While our results have established PABPC1 as a direct target of this complex and GPS2-mediated regulation, it is worth noting that the GPS2-regulated K63 ubiquitome included other putative targets involved in RNA processing and translation. As an example, we validated the eukaryotic translation initiation factor 3, subunit M (eIF3m), as an additional target of GPS2-mediated regulation and confirmed the expected increase in eIf3m ubiquitination in mitochondrial extracts from GPS2-KO cells (Supplemental Figure 4G). Thus, it is likely that ubiquitination of several factors may be affected by GPS2 deletion and contribute to regulate translation efficiency.

2.4. Remodeling of the mitochondrial proteome in the absence of GPS2

Recent studies have revealed an unexpected degree of specificity in the selection of transcripts that are translated on mitochondria-associated ribosomes in a coordinated manner with their mitochondrial import [12,14,16,18,20,62]. This suggested that GPS2-mediated regulation of mitochondrial translation may be impacting on a subset of nuclear-encoded genes rather than the entire mitochondrial proteome. To identify the targets of this regulatory strategy, we profiled the mitochondrial proteome of WT and KO MEF cells by mass spectrometry and integrated the results with the transcriptomic profile of mitochondria-associated mRNAs.

Profiling mitochondrial extracts from WT and KO MEFs using tandem mass tag (TMT) labeling followed by LC-MS/MS led to the identification of 858 differentially expressed proteins (DEPs) across three replicate experiments (Supplementary Table 2, P-value <0.05 and LogFC>0.25), including both mitochondrial (207 proteins as defined by inclusion in the Mitocarta 3.0 database [63]) and non-mitochondrial proteins. While this result may seem surprising considering that the purity of fractionated extracts is controlled for each sample by western blotting using markers of the different cellular compartments (Supplement Figure S5A), the identification of cytosolic proteins within mitochondrial extracts is to be expected considering: i) the sensitivity of the approach, ii) the tight association between mitochondrial membranes and other subcellular structures, and iii) the presence of cytosolic proteins known to interact with mitochondria [61–63]. Consistent with their localization, non-mitochondrial proteins were over-represented among upregulated DEPs which are enriched for broad cellular terms such as cell adhesion, cell cycle and protein folding and transport, and for pathways known to be regulated by cytosolic GPS2 [43,44,46,64] such as EGFR/Insulin signaling, inflammatory responses, and

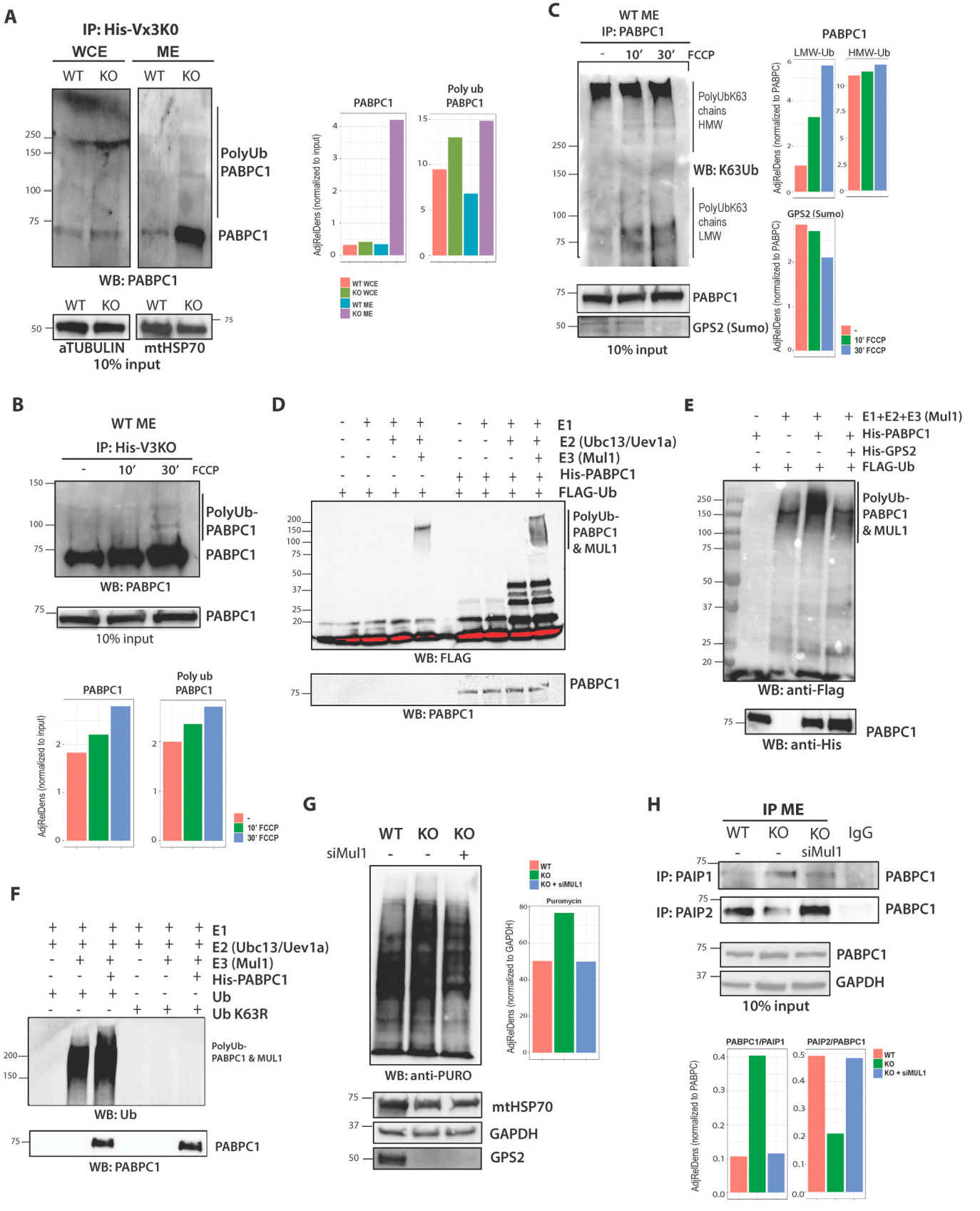

(caption on next page)

Fig. 4. GPS2 regulates the non-proteolytic ubiquitination of PABPC1 in mitochondria. A, Increased PABPC1 ubiquitination in in the absence of GPS2 is observed in mitochondrial extracts (ME) and not whole cell extracts (WCE) by IP with the K63-ubiquitin binding domain Vx3K0 and WB with PABPC1 antibody. Quantification of the blot by ORCA is normalized to GAPDH for ME and alpha-tubulin for WCE. B, Increased PABPC1 ubiquitination in response to FCCP treatment is observed in WT mitochondrial extracts (ME) by IP with the K63-ubiquitin binding domain Vx3K0 and WB with PABPC1 antibody. Quantification by ORCA is normalized to the PABPC1 input. C, Increased K63 ubiquitination of PABPC1 in WT MEFs mitochondrial extracts upon FCCP treatment is observed by IP/WB for PABPC/K63 Ub. Quantification by ORCA, performed separately for LMW chains (below 150kD) and HMW chains (above 150kD), is normalized by PABPC1 input. D, *In vitro* ubiquitination of PABPC1 by Ubc13/ MUL1 is visualized by WB for FLAG-Ub. E, *In vitro* ubiquitination of PABPC1 by Ubc13/ MUL1 is inhibited when recombinant GPS2 is added to the reaction. F, *In vitro* ubiquitination of PABPC1 with either WT Ub or K63R Ub is visualized by WB for Ub. G, Puromycin labeling of *de novo* protein synthesis in mitochondrial extracts from GPS2 WT, KO and KO with transient knockdown of MUL1 (siMul1) MEFs. Quantification of the blot by ORCA is normalized to GAPDH. H, Binding of PABPC1 with PAIP1 and PAIP2 in mitochondrial extracts from GPS2 WT, KO and KO with transient knockdown of MUL1 (siMul1) MEFs. Quantification of the blot by ORCA is normalized to the PABPC1 input.

TNFα/MAPK signaling (Supplemental Table 2 and Figure S5B). On the converse, GPS2 removal predominantly leads to defective mitochondrial gene expression as highlighted by a significant enrichment in mitochondria-related terms among pathways found enriched for downregulated DEPs across the entire dataset (Supplemental Figure S5B). This was expected based on GPS2 role as a required cofactor for the transcriptional activation of nuclear-encoded MITO genes, and consistent with previous results [9], downregulated proteins spanned across a variety of mitochondrial functions, including Electron Transport Chain (ETC), fatty acid oxidation, TCA cycle, and mitochondrial transport (Fig. 5A, Supplemental Figure S5B and Supplemental Table 2). Nonetheless, when focusing on the mitochondrial proteome, we identified a subset of mitochondrial proteins that are upregulated in the absence of GPS2, which includes proteins involved in the cellular response to stress and programmed cell death (Fig. 5A, Supplemental Figure S5C). To independently validate these results, we confirmed the downregulation of pyruvate dehydrogenase PDHA and OXPHOS proteins, and the upregulation of anti-oxidative factors SOD2 and PRDX2, and fatty acid synthase FASN by western blotting comparing mitochondrial extracts from GPS2 WT and KO MEFs (Fig. 5B).

Next, we profiled mitochondria-associated mRNAs from WT and GPS2-KO MEFs by RNA-seq to be able to integrate proteomic and transcriptomic data and dissect different level of regulation. Among the differentially expressed genes (DEGs), we identified 316 mitochondrial genes consistently regulated across three independent replicates, including 138 upregulated and 178 downregulated genes (Supplementary Table 3). Overlay of the RNA-seq results over the proteomics data confirmed that the downregulation of mitochondrial proteins observed in GPS2-KO cells is largely associated with reduced mRNA levels (Fig. 5**C,** left bottom quadrant), as expected based on GPS2 acting as a required transcriptional cofactor for the activation of neMITO genes [9]. Indeed, overlay of the MEFs proteomics data over GRO-seq data previously generated in 3T3-L1 cells with acute downregulation of GPS2 by siRNA further confirmed that protein downregulation likely results from defective transcription (Fig. 5**D,** left bottom quadrant) [9]. Mitochondrial proteins upregulated in GPS2-KO cells instead included genes presenting both increased (71 %, depicted in red in Fig. 5**C,** top right quadrant) or decreased (29 %, depicted in blue in Fig. 5**C,** top left quadrant) mRNA abundance in KO versus WT cells. However, comparison of protein and nascent RNA expression profilings indicates that the transcription of both up- and down-regulated mRNAs is impaired in the absence of GPS2 (Fig. 5**D**, most red proteins reside in the top left quadrant). This indicates that multiple levels of regulation contribute to the remodeling of the mitochondrial proteome of GPS2-KO cells, including transcriptional repression, post-transcriptional regulation of mRNA stability and protein synthesis, with the outcome for different gene/protein sets depending on the overlay of these complementary regulatory strategies.

To further investigate the relationship between GPS2-mediated regulation of mitochondria-associated translation and the post-transcriptional regulation of mitochondrial proteins found upregulated in GPS2-KO cells, we asked whether there was any previous evidence of their transcripts being co-translated at the site of import on the outer mitochondrial membrane. To address this question, we overlayed our data with previous studies unraveling the identity of RNA-binding proteins involved in targeting selected mRNAs to the OMM. In accord with our hypothesis, we observed that transcripts encoding for about 40 % of the mitochondrial proteins found upregulated in GPS2-KO cells are known to be recruited to the OMM for import-coupled translation via interaction with the AKAP1/MDI/LARP complex [18,65] (Supplementary Table 2). Conversely, only 1 protein is shared between upregulated proteins in the absence of GPS2 and transcripts binding to CluH, an RNA binding protein responsible for the assembly of cytosolic granules promoting the translation of a variety of mitochondrial proteins [15–17, 66], even though CluH-binding transcripts encode for several proteins showing reduced expression in the absence of GPS2 (Supplementary Table 2). Together, these comparative *in silico* analyses confirm that mitochondrial transcripts that are recruited to the OMM and translated by mitochondria-associated ribosomes are enriched among nuclear-encoded mitochondrial genes selectively upregulated at the protein level in GPS2 KO cells.

Based on these results, we conclude that GPS2 presence in mitochondria is important for the local regulation of import-coupled translation of selected neMITO transcripts and hypothesize that GPS2 retrograde translocation upon mitochondrial stress may promote their translation as part of the stress adaptive response. To address this hypothesis, we profiled the mitochondrial proteome from WT MEFs treated with FCCP, a mitochondrial stress inducer promoting GPS2 relocalization from mitochondria to the nucleus [9]. In accord with our previous data and with the literature [9,67], the FCCP-induced stress response promotes metabolic reprogramming, including changes in gene expression that support rewiring of both amino acid and lipid metabolism (Fig. 5E, Supplemental Table 4 and Supplemental Figure S5D). As expected, comparison of the two proteomics datasets (GPS2 WT/KO and WT+/-FCCP) confirmed that most of the FCCP-induced program is impaired in GPS2-KO cells, likely due to reduced transcription of stress response genes in the absence of nuclear GPS2 [9]. However, consistent among the datasets is the increased expression of the antioxidant gene expression program found regulated at the translational level in the absence of GPS2 (Fig. 5**E,** bottom cluster, Supplemental Table 4**,** genes highlighted in yellow). Among the putative targets of translational regulation, increased expression of antioxidant protein SOD2 upon FCCP stimulation was validated by western blotting (Supplemental Figure S5E). Together, these results indicate the complementarity of GPS2-mediated regulation of gene transcription and translation for a specific subset of nuclear-encoded mitochondrial genes that are activated as part of the adaptive response to mitochondrial stress.

3. Discussion

Previous studies have characterized GPS2 as a mediator of mitochondria retrograde signaling, a transcriptional cofactor involved in mediating both gene repression and activation, and an inhibitor of non-proteolytic K63 ubiquitination. Together, these complementary functions ensure a proper adaptive response to mitochondrial stress and regulate mitochondria biogenesis during differentiation, with GPS2 translocating from mitochondria to nucleus to regulate nuclear-encoded mitochondrial genes transcription via stabilization of chromatin

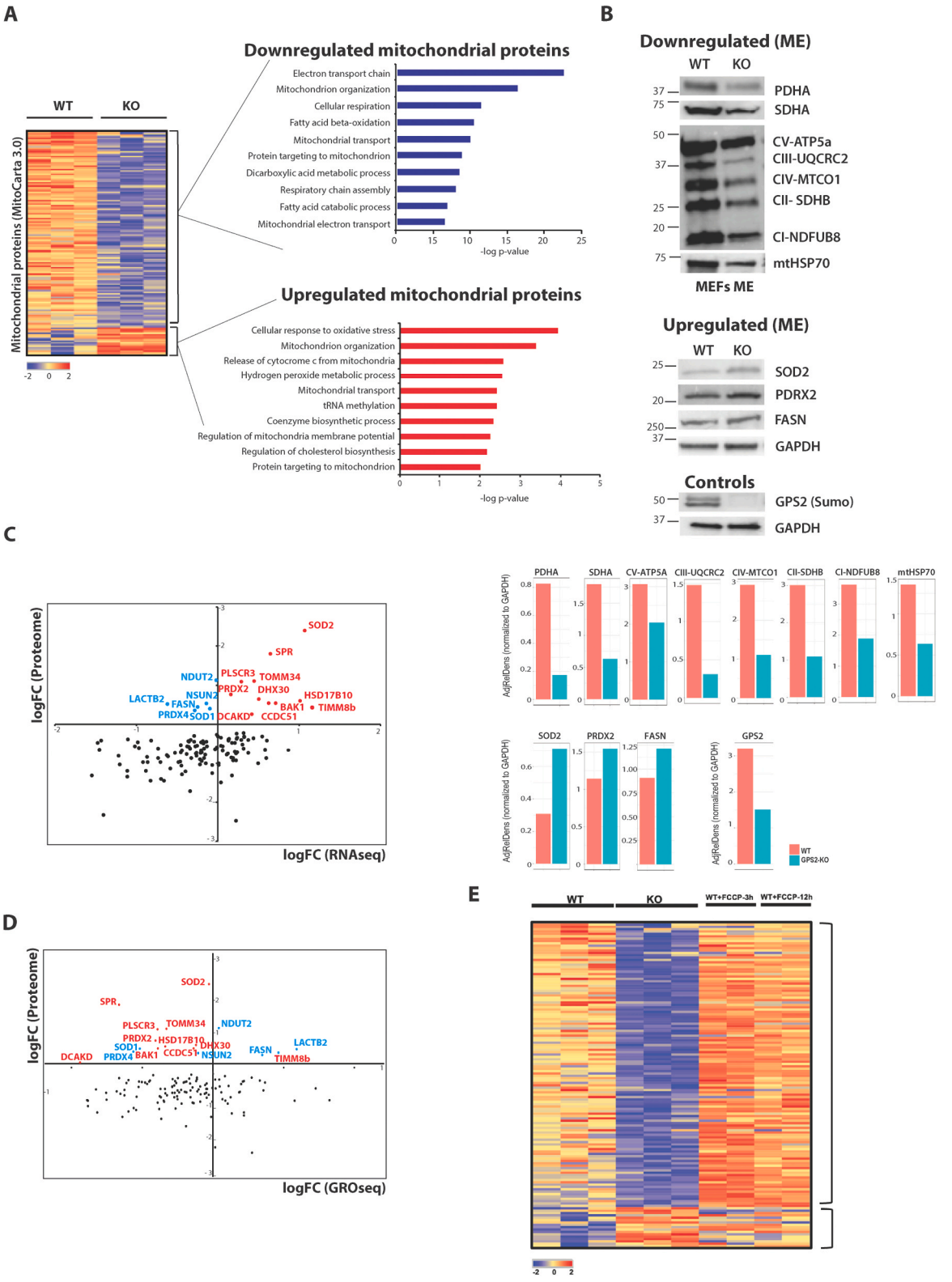

Fig. 5. Mitochondrial proteome remodeling in the absence of GPS2. A, Heatmap showing 207 differentially expressed mitochondrial proteins found by comparing GPS2 WT and KO MEFs by LC-MS/MS. The scale of heatmap color represents the log2 protein intensity. Enriched biological process GO terms of significantly downregulated (blue, upper panels) or upregulated (red, down panels) in response to GPS2 deficiency. B, Western blot analysis of representative mitochondrial proteins, including PDHA, SDHA, ETC proteins, mtHSP70, SOD2, PDRX2, and FASN normalized to GAPDH in mitochondrial extracts from WT and GPS2 KO MEFs. Quantification by ORCA is shown below. For each of the proteins analyzed by WB, quantification of the blot by ORCA is normalized to GAPDH. C&D, Distribution of 207 significantly changed mitochondrial proteins based on LC-MS/MS analysis and RNA-seq (C) or previously generated GRO-seq in 3T3-L1 cells [9](D). Red, upregulated proteins identified through RNA-seq and proteomics; Blue, upregulated proteins identified through proteomics, but downregulated in RNA-seq; Black, downregulated proteins identified through proteomics. E, Heatmap showing differentially expressed mitochondrial proteins (mitoDEPs) in GPS2 WT, KO MEFs and WT cells treated with FCCP for 3 h and 12 h. The scale of heatmap color represents the log2 protein intensity.

remodeling enzymes [9]. A key implication of these findings is that restricted K63 ubiquitination in the nucleus indirectly regulates mitochondrial functions through the expression of stress response and nuclear-encoded mitochondrial genes. However, it remains unclear whether GPS2 also contributes to the regulation of mitochondria homeostasis in a direct manner, possibly by modulating the ubiquitination of mitochondrial proteins. To address this question, we have profiled the GPS2-regulated K63 ubiquitome in mouse embryonic fibroblasts and human breast cancer cells. Our results confirm that there is a strong increase in the amount of K63 ubiquitination associated with mitochondria in GPS2-KO cells as compared to their WT counterpart. However, to our surprise, profiling of putative targets did not reveal any significant enrichment for classic mitochondrial proteins or overlap between the GPS2-regulated program and the mitochondrial proteins targeted by Parkin-mediated ubiquitination. This suggests that stress-induced translocation of GPS2 is unlikely to contribute to removing defective mitochondria via mitophagy. Instead, GPS2-mediated inhibition of K63 ubiquitination prevalently affects proteins involved in RNA processing and translation. In particular, our results indicate that GPS2-mediated inhibition of K63 ubiquitination contributes to regulating the mitochondria-associated translation of specific of nuclear-encoded mitochondrial genes on the outer mitochondrial membrane. Together with the previous characterization of nuclear GPS2 as an essential cofactor for the expression of nuclear-encoded mitochondrial genes, these findings indicate that GPS2-mediated inhibition of K63 ubiquitination represents a unifying strategy for modulating the expression of mitochondrial proteins through coordinated transcription and translation events.

To better appreciate how these processes are co-regulated through GPS2-mediated inhibition of K63 ubiquitination, it is important to consider that genetic manipulations to delete GPS2 results in the simultaneous removal of GPS2 activity across all subcellular compartments. This is distinct from what happens during an acute activation of the mitochondrial stress response, when GPS2 removal from mitochondria – via translocation from mitochondria to nucleus – is associated with an increase in nuclear GPS2 promoting the transcription of nuclear-encoded mitochondria and stress response genes. In the complete absence of GPS2, impaired nuclear transcription has a negative effect on mitochondrial biogenesis, with increased translation of selected mRNAs counteracting the oxidative stress caused by energetic imbalance. Upon acute mitochondria stress instead, GPS2 actions within different compartments cooperate in promoting the biogenesis of new, healthy mitochondria and reestablishing mitochondrial homeostasis, with the expression of selected antioxidant genes being supported at both the transcriptional and translational level.

Mitochondrial proteins regulated through this strategy are enriched for factors playing important antioxidant and detoxifying activities (SOD1/2, PRDX2/4, SPR, NUTD2), as well as proteins regulating mitochondrial RNA processing (LACTB2, NSUN2, HSD17b10), mitoribosome levels (DHX30) and protein import through the mitochondrial membrane (TOMM34, TIMM8b) [12,68–73]. This selective regulation of a protective gene expression program is consistent with both the role played by GPS2 in mediating the mitochondrial stress response (MSR) and the role played by K63 ubiquitination in regulating ribosomal activity in yeast [9,37,40,41]. Moreover, it is tempting to speculate that the localized modulation of factors involved in RNA processing and mitochondrial translation on organelles signaling to the nucleus may be relevant to understand why mitochondria translation preferentially occurs on mitochondria positioned within the peri-nuclear region [74]

Recent studies have identified RNA binding proteins, such as Puf3p in yeast, Clu and MDI/Larp in flies, CluH and dAKAP1/LARP4 in mammalian cells, that are involved in the selective regulation of different subsets of nuclear-encoded mitochondrial proteins [15,17,18,65,75–77]. Mitochondrial proteins upregulated in GPS2-KO cells are enriched for targets of the AKAP1/MDI/LARP complex, which recruits mRNAs to the OMM for import-coupled translation. In contrast, no significant overlap was observed with transcripts binding to CluH, an RNA binding protein responsible for the assembly of cytosolic granules promoting the cytosolic synthesis of various mitochondrial proteins. These results suggest that different sets of nuclear-encoded mitochondrial genes might be regulated through independent strategies, with GPS2-controlled K63 ubiquitination being restricted to the local regulation of mitochondria-associated translation. This separation is likely to be critical for ensuring the maintenance of mitochondrial and cellular homeostasis.

Mechanistically, our results indicate that GPS2 regulates mitochondrial-associated translation by inhibiting the ubiquitination of the RNA binding protein PABPC1, and possibly of other translation factors, by the mitochondrial E3 ubiquitin ligase MUL1. MUL1, also called MAPL, is a dual function E3 ligase promoting either the ubiquitination or SUMOylation of mitochondrial targets [78,79]. Previous studies have described an important role for MUL1 in regulating a variety of physiological and pathological processes, including mitochondrial dynamics, cell growth, apoptosis, and mitophagy [79–83]. Our study adds to this body of work by showing that MUL1-mediated ubiquitination regulates the activity of translation factors localized to the OMM and restricts the local translation of a subset of nuclear-encoded mitochondrial proteins. One intriguing aspect of MUL1 involvement in regulating mitochondria-associated translation is that it is uniquely suited for playing a key role in the mitochondrial stress response (MSR). Because of its spatial organization, MUL1 can in fact sense mitochondrial stress in the intermembrane mitochondrial space and respond through the ubiquitination of specific substrates on the outer mitochondrial surface [79,83,84]. Our data support this possibility as we observed increased ubiquitination of PABPC1 upon mitochondrial depolarization, concomitant to GPS2 retrograde translocation to the nucleus. Another intriguing aspect of MUL1 involment in this regulatory strategy is previous studies have reported MUL1 as repressing Parkin-mediated mitophagy [81,85]. Based on our results, it is tempting to speculate that there may be different waves of K63 ubiquitination events activated upon mitochondrial stress, with MUL1 activity being important for restraining mitophagy and promoting the activation of protective antioxidant genes when the stress is limited in time and/or intensity.

In conclusion, these results – together with the previous characterization of GPS2 as a required factor for the transcriptional activation of nuclear-encoded mitochondrial genes – uncover GPS2 as being crucial for the regulation of mitochondrial homeostasis through integration of different layers of gene expression regulation via modulation of ubiquitin signaling. While in this study we have mainly focused on PABPC1 as a key target of GPS2-regulated ubiquitination, our proteomics data suggest that there may be other targets relevant to the regulation of mitochondrial-associated translation, including known targets of ubiquitination, such as the eukaryotic translation initiation factor 3, subunit M (eIF3m), the ribosomal subunit RPS11 or scaffold factor RACK1. That ubiquitination of multiple targets may be involved in translational control is not surprising as several other examples of ubiquitin-related regulatory strategies have been reported [30,37,38]. However, it was unexpected to find that, in the context of mitochondrial-associated translation, increased ubiquitination promotes the synthesis of specific proteins rather than serving as a halting mechanism for global protein synthesis. Our results therefore reveal a more complex role for K63 ubiquitination than previously envisioned. We speculate that ubiquitination of different translation factors by specific machineries may have opposing functions and provide a strategy for facilitating the activation of stress response factors while other processes are shut down to preserve energy, in a similar fashion to the classic UPR response. As further studies will dissect the specific sites of ubiquitination and the contribution of individual PTM events to the regulation of translation across subcellular compartments, we will achieve a more complete understanding of these regulatory strategies and understand to which extent they can be modulated to improve cellular fitness.

4. Materials and methods

4.1. Reagents and antibodies

Anti-GPS2 antibody was generated in rabbit against a peptide representing aa 307–327. Commercial antibodies used were as follows: anti-ubiquitin (P4D1 clone, Cell Signaling Technology), anti-β-tubulin (TUB 2.1 clone, Sigma), anti-ATP5B (sc-55597, Santa Cruz Biotechnology), anti-HDAC2 (ab16032, Abcam), anti-mtHSP70 (catalog no. MA3–028, Invitrogen), anti-K63 (catalog no. 05–1308, Millipore), anti-α-Tubulin (catalog no. T5168, Sigma), anti-GAPDH (catalog no. MA5–15738, Invitrogen), anti-PABPC1 (ab21060, Abcam), anti-RPS11 (NBP2–22289, Novus Biologicals), anti-Rack1 (sc-17754, Santa Cruz Biotechnology), anti-eIF4G (15704–1-AP, Proteintech), anti-Paip1 (sc-365687, Santa Cruz Biotechnology), anti-Paip2 (15583–1-AP, proteintech), anti-Flag-HRP (catalog no. a8592, Sigma), anti-Puromycin (clone 12D10, Millipore), anti-PDHA (ab168379, Abcam), anti-Oxphos (ab110413, Abcam), anti-SOD2 (sc-137254, Santa Cruz Biotechnology).

4.2. Cell culture

Standard molecular cloning, cell culture, and cell transfection experiments were performed as described by J. Sambrook, D. W. Russell, Molecular Cloning: A Laboratory Manual (Cold Spring Harbor Laboratory Press, Cold Spring Harbor, N.Y., ed. 3rd, 2001). Immunostaining was performed following standard protocols on cells fixed in 4 % paraformaldehyde in PBS, using Alexa Fluor-conjugated secondary antibodies (Molecular probes).

Mouse embryonic fibroblasts (MEFs) cells were maintained in DMEM with 4.5 g/L glucose and L-glutamine and 10 % FBS at 37°C and 5 % CO_2. Conditional $Gps2^{flox/flox}$ mice were generated by inGenious Targeting Laboratory. Wild-type mice used as control for all analyses presented here were littermates $Gps2^{flox/flox/}CD19Cre^{-}$.

MDA-MB-231 breast cancer cells were grown in DMEM with 4.5 g/L glucose and L-glutamine and 10 % FBS at 37°C and 5 % CO_2. MDA-MB-231 GPS2 KO cells were generated and described previously [46].

4.3. Protein extraction, subcellular fractionation, immunoprecipitation and western blotting

For whole cell extraction, cultured cells were pelleted and incubated for 20 minutes on ice in IPH buffer (50 mM Tris HCl [pH 8.0], 250 mM NaCl, 5 mM EDTA, 0.5 % NP-40, 0.1 mM PMSF, 2 mM Na3VO4, 50 mM NaF, and 1X protease inhibitors (Sigma Aldrich)). For cytoplasmatic, mitochondrial and nuclear extracts fractionation, cells were rinsed in PBS, harvested and re-suspended in gradient buffer (10 mM HEPES pH 7.9, 1 mM EDTA, 210 mM Mannitol, 70 mM Sucrose, 10 mM NEM, 50 mM NaF, 2 mM Na2VO3, 1 mM PMSF and protease inhibitors cocktail), then homogenized via 10 passages through 25 G syringe followed by low-speed (300 g) centrifugation for 10 min. The nuclear pellet was incubated for 20 min in high-salt buffer (10 mM Hepes pH 7.9, 20 % glycerol, 420 mM NaCl, 1.5 mM MgCl2, 0.2 mM EDTA, 0.5 mM DTT, 10 mM NEM, 50 mM NaF, 2 mM Na2VO3, 1 mM PMSF and protease inhibitor mix) while the supernatant was recovered and subjected to high-speed centrifugation (9000 g) to separate the mitochondrial pellet from the cytoplasmic fraction. The mitochondrial pellet was incubated for 15 min in lysis buffer (50 mM Tris/HCl pH 8, 300 mM NaCl, 1 mM EDTA, 1 % Triton X-100, 10 mM NEM, 50 mM NaF, 2 mM Na2VO3, 1 mM PMSF and protease inhibitor mix). The concentration of protein extracts was measured using the Bradford assay (Bio-Rad). Extracts were boiled in SDS sample buffer and loaded directly on precast Bio-Rad gels. For immunoprecipitation, protein extracts were incubated with the specific antibody overnight at 4 °C after adjusting the buffer to a final concentration of 150 mM NaCl and 0.5 % NP-40 and then incubated for 1 h with Protein A-Sepharose™ 4B (Invitrogen), washed extensively, separated by electrophoresis, transferred onto PVDF membranes (Millipore), and subjected to Western blotting following standard protocols. Blots reported in the figures are representative of two or more experiments with comparable results. Individual blots were quantified using ORCA (OmniReprodubileCellAnalysis), a Shiny Application based in R, that provides a comprehensive tool for the semi-automated analysis of Western Blot (WB), Reverse Transcription-quantitative PCR (RT-qPCR), Enzyme-Linked ImmunoSorbent Assay (ELISA), Endocytosis and Cytotoxicity experiments [86]. For each experiment, ORCA generates a comprehensive report containing all the details about the analyses performed thus allowing for reproducible and detailed quantification of the proteins of interest. WB analysis is performed using two sequential modules. The Image Analysis module allows the user to select the bands of interest, generates densitometric curves, and calculates the Areas Under the Curve (AUC) for both the protein of interest and a normalizer. The Quantification module uses the results of the Image Analysis module in RDs (R Data Serialization) format for calculating the Relative Density (RD) and Adjusted Relative Density (AdjRD). ORCA reports for all blots are included in the Supplementary Data. More details and downloads are available at https://github.com/qBioTurin/ORCA/blob/main/README.md.

4.3.1. RNA extraction and qRT PCR analysis

Total RNA isolation was done using standard Trizol extraction. For qRT-PCRs, we reverse transcribed approximately 500 ng of total RNA from MEF cells silenced with either mock SiRNA or with target SiRNA using iScript Reverse Transcription Supermix with random primers (Biorad cat. #1708840) following manufacturer protocols. qPCR was performed on a Viaa7 termocycler using Fast SYBR Green master mix (applied biosystems, cat. #4385612). For mRNA fold change calculations, we used the $\Delta\Delta C_t$ method, normalized to the housekeeping gene *actin*. The following oligos were used for qRT-PCR:

Mouse UBC13-F: GCAGAACCAGATGAGAGCA
Mouse UBC13-R: AGTTTAAAAGTCCCTCCCTC
Mouse Mul1-F: GGAGCTAAGAAGATTCATCT
Mouse Mul1-R: TCCCCGGTGCTTCTGAAAG
Mouse Mkrn1-F: GTAGGAGCAGGTTCAGAGGA
Mouse Mkrn1-R: AGTGCAGGAAGGGGCAGTA
Mouse actin-F: CCTGACGGGCAGGTGATC
Mouse actin-R: ATGAAAGATGGCTGGAAGAGAGTCT

4.4. Recombinant protein expression

cDNAs encoding the tandem ubiquitin-binding entity (Vx3K0 and Rx3(A7) [49]) (Sims J., 2012, Nature protocol) were subcloned into pET28a-His-tag expression vector. His-tagged Vx3K0 and Rx3(A7) were produced as a His-tag fusion protein in BL21 *Escherichia coli*, resin-purified on nickel-nitrilotriacetic acid beads, and eluted accordingly to manufacturer's protocol (Life Technologies). The His-Vx3K0/Rx3(A7)-conjugated agarose were stored at 4°C in PBS supplemented with 30 % glycine.

4.5. Immunochemical methods

For pull-down of K63-ubiquitylated proteins, cells were lysed in high-stringency buffer (50 mM Tris, pH 7.5; 500 mM NaCl; 5 mM EDTA; 1 % NP40; 1 mM dithiothreitol (DTT); 0.1 % SDS) containing 1.25 mg ml−1 N-ethylmaleimide, 0.1 % PMSF, and protease inhibitor cocktail (Roche). His-Vx3K0/Rx3(A7) were added to immobilize the K63-ubiquitylated proteins, and bound material was washed extensively in high-stringency buffer four times. Proteins were resolved by SDS-PAGE and analyzed by immunoblotting.

4.6. Mitochondrial RNA Isolation and RNA-seq

Mitochondrial RNA was isolated from isolated mitochondrial pellet following the manufacturer protocol for the RNeasy Kit (QIAGEN).

Isolated mitochondrial RNA was subjected to quality control on Agilent Bioanalyzer and RNA library preparation following Illumina's RNA-seq Sample Preparation Protocol. Resulting cDNA libraries were sequenced on the Illumina's HiSeq 2000.

4.7. Mitochondrial content

Total DNA was extracted from cells using QuickExtract DNA Extraction Solution 1.0 (Epicenter) following manufacturer's instructions. DNA amplification of the mitochondrial-encoded NADH dehydrogenase 1 (mt-ND1) relative to nuclear TFAM was used to determine mitochondrial DNA copy number.

4.7.1. Translation activity

Puromycin incorporation into newly synthesized proteins was performed to measure translation activity. MEFs WT and GPS2-KO cells were treated in the presence or absence of homoharringtonine (HHT) (5 μM, Tocris Bioscience) for 10 min to prevent new translation initiation, prior to an additional 5 min incubation with puromycin (100 μM, Sigma) and emetine (200 μM, Sigma) at 37°C. Cells were collected by centrifugation, and lysate was prepared as described above. Thirty micrograms of protein were loaded onto a 10 % SDS-PAGE gel for immunoblotting analysis.

4.8. Sample preparation for MS analysis

For mitochondrial proteome profiling, mitochondrial proteins from MEFs WT and GPS2-KO cells were isolated as described before [9]. An equal amount of solubilized mitochondrial proteins from different samples were separated by SDS-PAGE and then digested in-gel by trypsin overnight using standard methods.

For SILAC-K63 experiments, MEFs WT and GPS2-KO cells or MDA-MB231 WT and GPS2-KO cells were grown in medium containing native (unlabeled) L-arginine and L-lysine (Arg0/Lys0) as the light condition, or stable isotope-labelled variants of L-arginine and L-lysine (Arg10/Lys8) as the heavy condition [87]. Proteins from whole cellular lysates were extracted from SILAC-labelled MEFs WT and GPS2-KO cells or MDA-MB-231WT and GPS2-KO cells as descripted before. An equal amount of protein from the two SILAC states was mixed and precipitated by His-Vx3K0-conjugated agarose and incubating at 4°C for 1 h. Precipitated proteins were eluted with SDS sample buffer, incubated with 10 mM DTT for 10 min at 100 °C. Proteins were separated by SDS-PAGE and then digested in-gel by trypsin overnight using standard methods. The resulting peptides were desalted using reverse phase (C18) Tips (Thermo Scientific) per the manufacturer's instructions.

For TMT based-K63 experiments, MEFs WT and GPS2-KO cells were grown in normal medium to 80 % confluency. After lysis with IPH buffer, protein quantities from whole cellular lysates were determined using the Bradford assay. An equal amount of protein from MEFs WT or GPS2-KO cells was precipitated by His-Vx3K0-conjugated agarose and incubating at 4°C for 1 h. Precipitated proteins were eluted with SDS sample buffer, incubated with 10 mM DTT for 10 min at 100 °C. Proteins were separated by SDS-PAGE and then digested in-gel by trypsin overnight using standard methods. The resulting peptides were desalted using C18 Tips (Thermo Scientific) per the manufacturer's instructions and vacuum-dried. The dried peptides were redissolved in 0.5 M TEAB, and processed independently according to the manufacturer's protocol for a 10-plex Tandem Mass Tag (TMT) reagent labeling kit (Thermo Fisher Scientific). The different TMT-labeled peptide mixtures were pooled equally, desalted and dried by vacuum centrifugation.

4.9. Mass spectrometric analysis

Peptides were analyzed on a Q-Exactive HF mass spectrometer (QE-HF, Thermo Fisher Scientific) equipped with a nanoflow EasyLC1200 HPLC system (Thermo Fisher Scientific). Peptides were loaded onto a C18 trap column (3 μm, 75 μm × 2 cm, Thermo Fisher Scientific) connected in-line to a C18 analytical column (2 μm, 75 μm × 50 cm, Thermo EasySpray) using the Thermo EasyLC 1200 system with the column oven set to 55 °C. The nanoflow gradient consisted of buffer A (composed of 2 % (v/v) ACN with 0.1 % formic acid) and buffer B (consisting of 80 % (v/v) ACN with 0.1 % formic acid). For protein analysis, nLC was performed for 180 min at a flow rate of 250 nL/min, with a gradient of 2–8 % B for 5 min, followed by a 8–20 % B for 96 min, a 20–35 % gradient for 56 min, and a 35–98 % B gradient for 3 min, 98 % buffer B for 3 min, 100–0 % gradient of B for 3 min, and finishing with 5 % B for 14 min. Peptides were directly ionized using a nanospray ion source and analyzed on the Q-Exactive HF mass spectrometer (Thermo Fisher Scientific).

QE-HF was run using data dependent MS2 scan mode, with the top 10 most intense precursor ions acquired per profile mode full-scan precursor mass spectrum subject to HCD fragmentation. Full MS spectra were collected at a resolution of 120,000 with an AGC of 3e6 or maximum injection time of 60 ms and a scan range of 350–1650 m/z, while the MS2 scans were performed at 45,000 resolutions, with an ion-packet setting of 2e4 for AGC, maximum injection time of 90 ms, and using 33 % NCE. Source ionization parameters were optimized with the spray voltage at 2.1 kV, transfer temperature at 275 °C. Dynamic exclusion was set to 40 seconds.

4.10. Data analysis

All acquired MS/MS spectra were searched against the Uniprot mouse complete proteome FASTA database released on 2013_07_01, using the MaxQuant software (Version 1.6.7.0) that integrates the Andromeda search engine. Enzyme specificity was set to trypsin and up to two missed cleavages were allowed. Cysteine carbamidomethylation was specified as a fixed modification. Methionine oxidation, N-terminal acetylation, and lysine ubiquitination were included as variable modifications. For SILAC data, the labeling of ^{13}C6-^{15}N2-lysine and ^{13}C6-^{15}N4-arginine were added as variable modifications. For TMT data, iTRAQ 10 plexes modification at the peptide N-terminus and lysine were set as variable modifications. Peptide precursor ions were searched with a maximum mass deviation of 6 ppm and fragment ions with a maximum mass deviation of 20 ppm. Peptide and protein identifications were filtered at 1 % FDR using the target-decoy database search strategy. Proteins that could not be differentiated based on MS/MS spectra alone were grouped to protein groups (default MaxQuant settings). For mitochondrial protein annotation, we utilized the latest Mitocarta dataset [63]. MaxQuant (Version 1.6.7.0) was used to quantify the proteins. *P-value* was calculated for significantly changed proteins in SILAC and TMT datasets. Only proteins with *P-value*<0.055 were considered as significantly changed proteins in proteome.

4.11. Statistical analysis

Statistical analysis was performed by the Student's t-test from three independent experiments for RT-qPCR and TMT-based quantification. SILAC experiments were performed in duplicate, RNAseq in quadruplicate. Results are shown as mean ± SEM unless mentioned otherwise.

4.12. Bioinformatics analysis

Differentially expressed proteins identified in this study were subjected to functional analyses using the Enrichr online platform, including Gene Ontologies and pathways analyses [88–90]. The background of KEGG analysis is the whole theoretical genome.

Author contributions

The study was conceived and designed by Y.G., M.D.C. and V.P. with intellectual contributions by S.M.L. Data collection, analysis and figure

preparation was performed by Y.G., J.K., J.O., G.B., S.M., T.F., J.E. and R.H. with supervision by A.E., M.D.C. and V.P. The manuscript was prepared by Y.G. and V.P. with feedback and assistance by all other authors.

Funding

This work was supported by National Institutes of Health and Department of Defense grant awards as follows: NIGMS R01 GM127625 and R35 GM149339 to VP, DoD W81XWH-17-1-0048 to VP, R00GM124458 to SML.

CRediT authorship contribution statement

Yuan Gao: Writing – review & editing, Writing – original draft, Methodology, Investigation, Conceptualization. **Valentina Perissi:** Writing – review & editing, Writing – original draft, Supervision, Project administration, Funding acquisition, Conceptualization. **Julian Kwan:** Methodology, Investigation, Formal analysis. **Shawn Lyons:** Writing – review & editing, Conceptualization. **Maria Dafne Cardamone:** Writing – review & editing, Supervision, Conceptualization. **Ryan Hekman:** Investigation. **Andrew Emili:** Supervision, Resources. **Ting-Yu Fan:** Investigation. **Justin English:** Writing – review & editing, Investigation. **Giulia Burrone:** Writing – review & editing, Visualization. **Sahana Mitra:** Writing – review & editing, Validation, Investigation. **Joseph Orofino:** Formal analysis.

Declaration of Competing Interest

The authors declare that they have no known competing financial interests or personal relationships that could have appeared to influence the work reported in this paper.

Data availability

The mass spectrometry proteomics data have been deposited to the ProteomeXchange Consortium via the PRIDE partner repository with the dataset identifier PXD030187.

Acknowledgments

We thank all past and present members of the Perissi Lab for their continuous support and fruitful discussions, and Christian Heckendorf and Carl White in the Emili lab for assistance with data submission to the ProteomeXchange. We are also grateful to Drs. Christine Vogel (NYU) and Gustavo M. Silva (Duke University) for their assistance with protocols for the enrichment of K63 ubiquitinated proteins; to Prof. Ping Xu (State Key Laboratory of Proteomics, Beijing Proteome Research Center, China) for help with the analysis of proteomics data; and to Drs. Francesca Cordero, Simone Pernice and Dora Tortarolo (University of Torino, Italy) for assistance and training in the use of OmniR-eprodubileCellAnalysis (ORCA) for data quantification. Genomic profiling experiments have been run by the Boston University Microarray & Sequencing Resource Core. The graphical abstract was created with BioRender.com.

Appendix A. Supporting information

Supplementary data associated with this article can be found in the online version at doi:10.1016/j.phrs.2024.107336.

References

[1] K. Palikaras, N. Tavernarakis, Mitochondrial homeostasis: the interplay between mitophagy and mitochondrial biogenesis, Exp. Gerontol. 56 (2014) 182–188.
[2] P.M. Quirós, A. Mottis, J. Auwerx, Mitonuclear communication in homeostasis and stress, Nat. Rev. Mol. Cell Biol. 17 (2016) 213–226.
[3] I. RS, M. E, C. LS, The multiple levels of mitonuclear coregulation, Annu Rev. Genet 52 (2018) 511–533.
[4] J. English, J.M. Son, M.D. Cardamone, C. Lee, V. Perissi, Decoding the rosetta stone of mitonuclear communication, Pharm. Res (2020) 105161, https://doi.org/10.1016/j.phrs.2020.105161.
[5] J.D. Woodson, J. Chory, Coordination of gene expression between organellar and nuclear genomes (Preprint at), Nat. Rev. Genet. vol. 9 (2008) 383–395, https://doi.org/10.1038/nrg2348.
[6] C.J. Fiorese, et al., The transcription factor ATF5 mediates a mammalian mitochondrial UPR, Curr. Biol. 26 (2016) 2037–2043.
[7] N. AM, P. MW, F. CJ, B. BM, H. CM, Mitochondrial import efficiency of ATFS-1 regulates mitochondrial UPR activation, Science 337 (2012) 587–590.
[8] A. S, et al., MNRR1 (formerly CHCHD2) is a bi-organellar regulator of mitochondrial metabolism, Mitochondrion 20 (2015) 43–51.
[9] M.D. Cardamone, et al., Mitochondrial retrograde signaling in mammals is mediated by the transcriptional cofactor GPS2 via direct mitochondria-to-nucleus translocation, Mol. Cell 69 (2018) 757–772.e7.
[10] C. MT, S. IC, S. G, C. LS, Synchronized mitochondrial and cytosolic translation programs, Nature 533 (2016) 499–503.
[11] A. Margeot, et al., Why are many mRNAs translated to the vicinity of mitochondria: a role in protein complex assembly, Gene 354 (2005) 64–71.
[12] A. Chacinska, et al., Importing mitochondrial proteins: machineries and mechanisms, Cell 138 (2009) 628–644.
[13] Y.S. Bykov, D. Rapaport, J.M. Herrmann, M. Schuldiner, Cytosolic Events in the Biogenesis of Mitochondrial Proteins, Trends Biochem Sci. 45 (2020) 650–667.
[14] D. Schatton, E.I. Rugarli, A concert of RNA-binding proteins coordinates mitochondrial function, Crit. Rev. Biochem Mol. Biol. 53 (2018) 652–666.
[15] D. Pla-Martín, et al., CLUH granules coordinate translation of mitochondrial proteins with mTORC1 signaling and mitophagy, EMBO J. 39 (2020).
[16] J. Gao, et al., CLUH regulates mitochondrial biogenesis by binding mRNAs of nuclear-encoded mitochondrial proteins, J. Cell Biol. 207 (2014) 213–223.
[17] D. Schatton, et al., CLUH regulates mitochondrial metabolism by controlling translation and decay of target mRNAs, J. Cell Biol. 216 (2017) 675–693.
[18] Z. Y, C. Y, G. M, X. H, The mitochondrial outer membrane protein MDI promotes local protein synthesis and mtDNA replication, EMBO J. 35 (2016) 1045–1057.
[19] S. A, C. RT, Clueless is a conserved ribonucleoprotein that binds the ribosome at the mitochondrial outer membrane, Biol. Open 5 (2016) 195–203.
[20] L.J. García-Rodríguez, et al., Puf3p, a Pumilio family RNA binding protein, localizes to mitochondria and regulates mitochondrial biogenesis and motility in budding yeast, J. Cell Biol. 176 (2007) 197–207.
[21] C.C. Williams, et al., Targeting and plasticity of mitochondrial proteins revealed by proximity-specific ribosome profiling, Science (1979) 346 (748–751) (2014).
[22] M. Garcia, et al., Mitochondria-associated yeast mRNAs and the biogenesis of molecular complexes, Mol. Biol. Cell 18 (2006) 362–368.
[23] P. CM, Mechanisms underlying ubiquitination, Annu Rev. Biochem 70 (2001) 503–533.
[24] B. CE, W. C, New insights into ubiquitin E3 ligase mechanism, Nat. Struct. Mol. Biol. 21 (2014) 301–307.
[25] Y. Kravtsova-Ivantsiv, A. Ciechanover, Non-canonical ubiquitin-based signals for proteasomal degradation, J. Cell Sci. 125 (2012) 539–548.
[26] A. M, D. I, B. A, Ubiquitin chain diversity at a glance, J. Cell Sci. 129 (2016) 875–880.
[27] I. F, C. N, D. I, What determines the specificity and outcomes of ubiquitin signaling, Cell 143 (2010) 677–681.
[28] Z.J. Chen, L.J. Sun, Nonproteolytic functions of ubiquitin in cell signaling, Mol. Cell 33 (2009) 275–286.
[29] D. Mukhopadhyay, H. Riezman, Proteasome-independent functions of ubiquitin in endocytosis and signaling, Science 315 (201–205) (1979) 2007.
[30] S. J, et al., Cell cycle-regulated modification of the ribosome by a variant multiubiquitin chain, Cell 102 (2000) 67–76.
[31] H. F, et al., Lysine 63-linked polyubiquitination is required for EGF receptor degradation, Proc. Natl. Acad. Sci. USA 110 (2013) 15722–15727.
[32] L. E, J. C, A. B, K63-linked ubiquitin chains as a specific signal for protein sorting into the multivesicular body pathway, J. Cell Biol. 185 (2009) 493–502.
[33] S. GS, et al., The RIDDLE syndrome protein mediates a ubiquitin-dependent signaling cascade at sites of DNA damage, Cell 136 (2009) 420–434.
[34] D. C, et al., RNF168 binds and amplifies ubiquitin conjugates on damaged chromosomes to allow accumulation of repair proteins, Cell 136 (2009) 435–446.
[35] H. C, P. B, M. GL, P. G, J. S, RAD6-dependent DNA repair is linked to modification of PCNA by ubiquitin and SUMO, Nature 419 (2002) 135–141.
[36] G. MU, et al., TRIM25 RING-finger E3 ubiquitin ligase is essential for RIG-I-mediated antiviral activity, Nature 446 (2007) 916–920.
[37] S. GM, F. D, V. C, K63 polyubiquitination is a new modulator of the oxidative stress response, Nat. Struct. Mol. Biol. 22 (2015) 116–123.
[38] S.E. Dougherty, A.O. Maduka, T. Inada, G.M. Silva, Expanding role of ubiquitin in translational control, Int J. Mol. Sci. 21 (2020).
[39] P. IC, S. W, Functional implications of K63-linked ubiquitination in the iron deficiency response of Arabidopsis roots, Front Plant Sci. (4) (2014).
[40] S. Back, A.W. Gorman, C. Vogel, G.M. Silva, Site-Specific K63 Ubiquitinomics Provides Insights into Translation Regulation under Stress, J. Proteome Res 18 (2019) 309–318.
[41] Y. Zhou, et al., Structural impact of K63 ubiquitin on yeast translocating ribosomes under oxidative stress, Proc. Natl. Acad. Sci. USA 117 (2020) 22157–22166.
[42] W. L, et al., Arabidopsis UBC13 differentially regulates two programmed cell death pathways in responses to pathogen and low-temperature stress, N. Phytol. 221 (2019) 919–934.

[43] C. Lentucci, et al., Inhibition of Ubc13-mediated Ubiquitination by GPS2 Regulates Multiple Stages of B Cell Development, J. Biol. Chem. 292 (2017).
[44] C.T. Cederquist, et al., Systemic insulin sensitivity is regulated by GPS2 inhibition of AKT ubiquitination and activation in adipose tissue, Mol. Metab. 6 (2017) 125–137.
[45] M. Cardamone, et al., A protective strategy against hyperinflammatory responses requiring the nontranscriptional actions of GPS2, Mol. Cell 46 (2012).
[46] S. Chan, et al., Loss of G-protein pathway suppressor 2 promotes tumor growth through activation of AKT signaling, Front Cell Dev. Biol. 8 (2021).
[47] M. Cardamone, et al., GPS2/KDM4A pioneering activity regulates promoter-specific recruitment of PPARγ, Cell Rep. 8 (2014).
[48] K. Drareni, et al., GPS2 deficiency triggers maladaptive white adipose tissue expansion in obesity via HIF1A activation, Cell Rep. 24 (2018) 2957–2971.e6.
[49] J.J. Sims, et al., Polyubiquitin-sensor proteins reveal localization and linkage-type dependence of cellular ubiquitin signaling, Nat. Methods 9 (2012) 303.
[50] A. Ordureau, et al., Dynamics of PARKIN-dependent mitochondrial ubiquitylation in induced neurons and model systems revealed by digital snapshot proteomics, Mol. Cell 70 (2018) 211–227.e8.
[51] R.J. Youle, D.P. Narendra, Mechanisms of mitophagy, *2011 12*, Nat. Rev. Mol. Cell Biol. *1* (12) (2010) 9–14.
[52] A. Hildebrandt, et al., The RNA-binding ubiquitin ligase MKRN1 functions in ribosome-associated quality control of poly(A) translation, Genome Biol. *1* (20) (2019) 1–20.
[53] B. F, et al., Comprehensive analysis of the ubiquitinome during oncogene-induced senescence in human fibroblasts, Cell Cycle 14 (2015) 1540–1547.
[54] M. Wetzler, D. Segal, Omacetaxine as an anticancer therapeutic: what is old is new again, Curr. Pharm. Des. 17 (2011) 59–64.
[55] N. Sonenberg, A.G. Hinnebusch, Regulation of Translation Initiation in Eukaryotes: Mechanisms and Biological Targets, Cell 136 (2009) 731.
[56] K. A, S. YV, S. R, M. MN, S. N, Mammalian poly(A)-binding protein is a eukaryotic translation initiation factor, which acts via multiple mechanisms, Genes Dev. 19 (2005) 104–113.
[57] M. Yoshida, et al., Poly(A) binding protein (PABP) homeostasis is mediated by the stability of its inhibitor, Paip2, EMBO J. 25 (2006) 1934.
[58] Z. Wu, et al., Ubiquitination of ABCE1 by NOT4 in response to mitochondrial damage links co-translational quality control to PINK1-directed mitophagy, Cell Metab. 28 (2018) 130–144.e7.
[59] N. Zemirli, et al., Mitochondrial hyperfusion promotes NF-κB activation via the mitochondrial E3 ligase MULAN, FEBS J. 281 (2014) 3095–3112.
[60] G. Ni, H. Konno, G.N. Barber, Ubiquitination of STING at lysine 224 controls IRF3 activation, Sci. Immunol. 2 (2017).
[61] X. Calle, et al., Mitochondrial E3 ubiquitin ligase 1 (MUL1) as a novel therapeutic target for diseases associated with mitochondrial dysfunction, IUBMB Life 74 (2022) 850–865.
[62] S. Gehrke, et al., PINK1 and parkin control localized translation of respiratory chain component mRNAs on mitochondria outer membrane, Cell Metab. 21 (2015) 95–108.
[63] S. Rath, et al., MitoCarta3.0: an updated mitochondrial proteome now with sub-organelle localization and pathway annotations, Nucleic Acids Res 49 (2021) D1541.
[64] Y. Si, et al., G protein pathway suppressor 2 suppresses gastric cancer by destabilizing epidermal growth factor receptor, Cancer Sci. (2021), https://doi.org/10.1111/CAS.15151.
[65] L. Gabrovsek, et al., A-kinase-anchoring protein 1 (dAKAP1)-based signaling complexes coordinate local protein synthesis at the mitochondrial surface, J. Biol. Chem. 295 (2020) 10749–10765.
[66] P.-M. D, et al., CLUH granules coordinate translation of mitochondrial proteins with mTORC1 signaling and mitophagy, EMBO J. 39 (2020).
[67] P.M. Quirós, et al., Multi-omics analysis identifies ATF4 as a key regulator of the mitochondrial stress response in mammals, J. Cell Biol. 216 (2017) 2027–2045.
[68] Z.A. Wood, E. Schröder, J.R. Harris, L.B. Poole, Structure, mechanism and regulation of peroxiredoxins, Trends Biochem Sci. 28 (2003) 32–40.
[69] A. Biosa, et al., Superoxide dismutating molecules rescue the toxic effects of PINK1 and parkin loss, Hum. Mol. Genet 27 (2018) 1618.
[70] V. Zegarra, C.-N. Mais, J. Freitag, G. Bange, The mysterious diadenosine tetraphosphate (AP4A), microLife 4 (2023) 1–8.
[71] L. Gao, et al., Sepiapterin reductase regulation of endothelial tetrahydrobiopterin and nitric oxide bioavailability, Am. J. Physiol. Heart Circ. Physiol. 297 (2009) 331–339.
[72] L. Van Haute, et al., NSUN2 introduces 5-methylcytosines in mammalian mitochondrial tRNAs, Nucleic Acids Res 47 (2019) 8720–8733.
[73] S. Levy, et al., Identification of LACTB2, a metallo-β-lactamase protein, as a human mitochondrial endoribonuclease, Nucleic Acids Res 44 (2016) 1813.
[74] C.A. Albus, et al., Mitochondrial Translation Occurs Preferentially in the Peri-Nuclear Mitochondrial Network of Cultured Human Cells, Biol. (Basel) (10) (2021).
[75] K. Schäffler, et al., A stimulatory role for the La-related protein 4B in translation, Rna 16 (2010) 1488–1499.
[76] C. Lesnik, A. Golani-Armon, Y. Arava, Localized translation near the mitochondrial outer membrane: an update, RNA Biol. 12 (2015) 801–809.
[77] E. Eliyahu, et al., Tom20 mediates localization of mRNAs to mitochondria in a translation-dependent manner, Mol. Cell Biol. 30 (2010) 284–294.
[78] B. E, Z. R, M. HM, MAPL is a new mitochondrial SUMO E3 ligase that regulates mitochondrial fission, EMBO Rep. 10 (2009) 748–754.
[79] J. Peng, K. Ren, J. di, Yang, X.J. Luo, Mitochondrial E3 ubiquitin ligase 1: A key enzyme in regulation of mitochondrial dynamics and functions, Mitochondrion 28 (2016) 49–53.
[80] E.-H. M, J. M, Mitofusins: disease gatekeepers and hubs in mitochondrial quality control by E3 ligases, Front Physiol. (10) (2019).
[81] P. R, C. XT, L. MY, H. N, S. ZH, Mul1 restrains Parkin-mediated mitophagy in mature neurons by maintaining ER-mitochondrial contacts, Nat. Commun. (10) (2019).
[82] P. R, C. XT, L. MY, H. N, S. ZH, Defending stressed mitochondria: uncovering the role of MUL1 in suppressing neuronal mitophagy, Autophagy 16 (2020) 176–178.
[83] A. Neutzner, G. Benard, R.J. Youle, M. Karbowski, Role of the ubiquitin conjugation system in the maintenance of mitochondrial homeostasis, Ann. N. Y Acad. Sci. 1147 (2008) 242–253.
[84] L. W, et al., Genome-wide and functional annotation of human E3 ubiquitin ligases identifies MULAN, a mitochondrial E3 that regulates the organelle's dynamics and signaling, PLoS One 3 (2008).
[85] R. Puri, X.T. Cheng, M.Y. Lin, N. Huang, Z.H. Sheng, Defending stressed mitochondria: uncovering the role of MUL1 in suppressing neuronal mitophagy, Autophagy 16 (2020) 176–178.
[86] D. Tortarolo, et al., OmniReprodubileCellAnalysis: a comprehensive toolbox for the analysis of cellular biology data, 2023 IEEE Int. Conf. Bioinforma. Biomed. (BIBM) (2023) 3748–3755, https://doi.org/10.1109/BIBM58861.2023.10385438.
[87] S.E. Ong, et al., Stable isotope labeling by amino acids in cell culture, SILAC, as a simple and accurate approach to expression proteomics, Mol. Cell Proteom. 1 (2002) 376–386.
[88] Z. Xie, et al., Gene set knowledge discovery with enrichr, Curr. Protoc. 1 (2021) e90.
[89] E.Y. Chen, et al., Enrichr: interactive and collaborative HTML5 gene list enrichment analysis tool, BMC Bioinforma. 14 (2013) 128.
[90] M.V. Kuleshov, et al., Enrichr: a comprehensive gene set enrichment analysis web server 2016 update, Nucleic Acids Res 44 (2016) W90.
[91] C. Tristan, N. Shahani, T.W. Sedlak, A. Sawa, The diverse functions of GAPDH: Views from different subcellular compartments, Cell Signal 23 (2011) 317–323.
[92] H. Nakajima, et al., Glyceraldehyde-3-phosphate dehydrogenase (GAPDH) aggregation causes mitochondrial dysfunction during oxidative stress-induced cell death, J. Biol. Chem. 292 (2017) 4727–4742.